Polymer Testing 81 (2020) 106219

Contents lists available at ScienceDirect

Polymer Testing

journal homepage: http://www.elsevier.com/locate/polytest

High strain rate behavior of graphene-epoxy nanocomposites

Özgen U. Colak [a,b,*], Nadia Bahlouli [b], Deniz Uzunsoy [c], Charles Francart [b]

[a] Yıldız Technical University, Department of Mechanical Engineering, Istanbul, Turkey
[b] ICUBE, Université de Strasbourg/CNRS, Strasbourg, France
[c] Bursa Technical University, Department of Metallurgy & Materials Engineering, Turkey

ARTICLE INFO

Keywords:
Graphene-epoxy nanocomposite
Split hopkinson bar
Compression test
Electric arc discharge technique

ABSTRACT

This work consists of the synthesis of high purity graphene nanoflakes (GNF), the manufacturing of GNF-epoxy nanocomposites and the mechanical characterization of the nanocomposite at high and quasi static strain rates, (2750/s - 1.E−5/s). GNF were synthesized by using the electric arc discharge technique. Thermogravimetry/Differential Thermal Analysis (TG/DTA) of synthesized graphene reveals high purity and high crystallinity. Raman spectra and the broad Brunauer-Emmet-Teller (BET) specific surface area indicate that the synthesized graphene has several layers. Following the solution mixing manufacturing process of GNF-epoxy nanocomposites, the influences of strain rate on the mechanical behaviors are investigated under quasi static and dynamic loadings. High strain rate uniaxial compression tests (1270–2750/s) using Split Hopkinson Pressure Bar (SHPB) and quasi static compression tests (1.E−3 and 1.E−5/s) of GNF-epoxy with two graphene contents (0.1 and 0.5 wt %) are performed at room temperature. The maximum elasticity modulus achieved by the GNF-epoxy with 0.5 wt% at the strain rate of 2350/s corresponds to a 68% increase compared to the neat epoxy. The yield strength of the material is doubled under dynamic loading conditions compared to the quasi static loading.

1. Introduction

High strain rate deformations of the materials are observed in a variety of applications such as crash of vehicles, bullet proof armors and impact of the structures. On the other hand, forming processes like extrusion and rolling can also result in high strain rate deformation. In the design and analysis of the structural components which are under the effect of dynamic loading, the high strain rate data are required for safety and structural integrity. A deep understanding about the effect of strain rate on the material properties is crucial in the design and safe in-service performance of polymeric structural components.

Polymers and composites exhibit rate dependent behavior even at room temperature. Strain rate has been known to affect the mechanical behavior of polymers quite significantly. Their behavior in quasi static and dynamic loading rates are quite different. Low strain rate tests are referred to as isothermal since the heat generated during plastic deformation is dissipated before any significant temperature increase is observed in the material. At the strain rates of 10/s or greater, the heat generated due to plastic deformation does not have time to dissipate and results in a temperature increase; these tests are referred to as adiabatic tests. Adiabatic heating can result in strain localization and may also bring about some microstructural changes [1,2].

In order to provide the industrial applications of graphene, it is necessary to shorten the manufacturing process, to produce the graphene with a large scale and high purity and to characterize the graphene reinforced nanocomposites at different loading conditions. Graphene can be obtained by many different production methods. These are; electrochemical exfoliation, solvent based exfoliation, reduction of graphene oxide, chemical vapor deposition and electric arc discharge methods [3–7]. Some of these methods contain intensive chemical processes. This situation causes defects in the structure and decreases the rate of crystallization. Compared to the other methods, graphene obtained by electric arc discharge method has many advantages such as low cost production, high efficiency and synthesis opportunity without any catalysis usage [6,8]. In this work, high purity several-layer graphene is produced by using electric arc discharge method and the solution mixing method was used for the preparation of GNF-epoxy nanocomposites.

Recent researches on the graphene-epoxy nanocomposites have focused on fabrication and characterization at quasi-static loadings

* Corresponding author. Yıldız Technical University, Department of Mechanical Engineering, Istanbul, Turkey.
E-mail addresses: ozgen@yildiz.edu.tr (Ö.U. Colak), nadia.bahlouli@unistra.fr (N. Bahlouli), deniz.uzunsoy@btu.edu.tr (D. Uzunsoy), cfrancart@unistra.fr (C. Francart).

https://doi.org/10.1016/j.polymertesting.2019.106219
Received 10 July 2019; Received in revised form 7 November 2019; Accepted 9 November 2019
Available online 9 November 2019

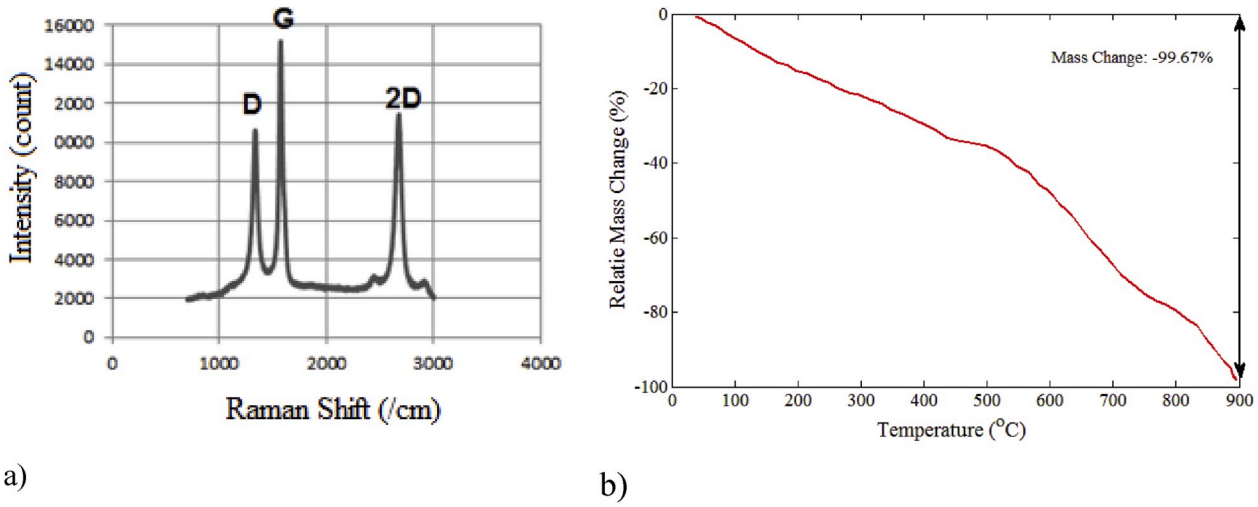

Fig. 1. a) Raman spectra of synthesized graphene samples at the electrode diameter of 12 mm and the arc current of 150 A in a He and N_2 atmosphere. b) TG/DTA analysis of GNF.

[9–11]. In the literature, high strain rate behavior of graphene-epoxy nanocomposites are not investigated. Most of the works about high strain rate are about epoxy based nanocomposites with different reinforcements such as clay and silica [12–15], but not graphene. Gurusideswar et al. [12] investigated the effect of medium strain rate on the tensile behavior of epoxy/clay nanocomposites which is fabricated using the mechanical stirrer. Dynamic tensile characterization of epoxy/clay nanocomposites at the strain rates from quasi-static to 445/s is carried out on drop mass setup and Digital Image Correlation (DIC) technique. It is observed that tensile strength and the modulus increase with an increase in the strain rate for epoxy and its clay nanocomposites.

Tian et al. [13] investigated the strain-rate effect (0.001–3000/s) on the compressive properties of epoxy and the epoxy filled with sol-gel-formed silica nanoparticles. At low, intermediate and high strain rates, the experiments are performed. When the strain rate is increased, the compressive modulus and transition strength increased, the strain at break and ultimate strength decreased more or less, while the strain energy at fracture nearly did not change.

In the work by Shadlou et al. [9], the influences of strain rate on the mechanical behavior of epoxy reinforced with graphene nanoplatelets (GNPs) are investigated under quasi static compressive and tensile loadings. A soft molding method is used for the preparation of epoxy nanocomposites by Topal et al. [11]. The reinforcing effects of GNP and the reduced graphene oxide (R-GO) on epoxy resin are examined by tensile testing and dynamic mechanical analysis (DMA). It is observed that the ultimate tensile strength has decreased, although the elasticity modulus has improved.

The detailed literature review reveals that the work by Bansal et al. [16] is the only work about high strain rate of graphene oxide (GO)-epoxy nanocomposite. They investigated the impact loading response of GO reinforced epoxy nanocomposites up to 1000/s of high strain rate. In the strain rate range of 600–815/s, the strength of GO-epoxy with 0.5 wt % of the nanofiller has improved by 41% compared to the epoxy.

The purpose of this work is three fold: synthesis of high purity graphene nanoflakes (GNF), manufacturing of GNF-epoxy nanocomposite and investigation of GNF-epoxy nanocomposite and pure epoxy under quasi static and high strain rate loadings. In this work, GNFs were synthesized using electric arc discharge method. The purity and the number of layers of graphene were determined via TG/DTA, BET, the Raman spectroscopy and Transmission Electron Microscopy (TEM) respectively. GNFs obtained at the arc current of 150 A in a He and N_2 atmosphere were used for the manufacturing of nanocomposites. The method for manufacturing GNF-epoxy nanocomposites is the commonly-used solution mixing technique. TG/DTA graph of graphene reveals high purity and high crystallinity. Raman spectra and the broad BET specific surface area indicate that the synthesized graphene has several layers. Apart from many works in the literature, both the synthesis of GNFs and the manufacturing of nanocomposite are done along with the determination of the mechanical properties under quasi static and dynamic loading. The main uniqueness of the present work is the investigation of high strain rate of GNF-epoxy nanocomposite and epoxy along with quasi static behavior. The influences of strain rate on the mechanical behaviors are investigated. Quasi static (1.E−3 and 1.E−5/s) and high strain rate uniaxial compression tests (1270–2750/s) of GNF-epoxy with two graphene contents (0.1 and 0.5 wt %) are performed at room temperature. Dynamic uniaxial compression tests of GNF-epoxy with two graphene contents were performed on Split Hopkinson Pressure Bar (SHPB). Increased mechanical properties at yield strength and elasticity modulus were observed at GNF-epoxy with 0.1 and 0.5 wt% at high strain rates loadings. At the strain rate of 2350/s, the maximum strength achieved by the GNF-epoxy with 0.5 wt% correspond to a 12.5% increase compared to the neat epoxy. 68.2% increase in the elasticity modulus compared to the neat epoxy is obtained for GNF-epoxy with 0.5 wt % at the strain rate of 2350/s. The yield strength of the nanocomposite is almost doubled at high strain rates compared to the quasi static loading.

2. Synthesis of graphene nanoflakes

Electric arc discharge method based on the principle that provides a constant current between two high purity graphite electrodes to vaporize is used for the synthesis of GNF, [17,18]. After the arc discharge, nanoparticles accumulate on the inner surface of the home-made reactor. High purity graphite rods (99.9%) with a diameter of 10 mm and 12 mm are used as electrodes. Reactor is kept under pressure for approximately 5 min. In the electric arc discharge method, the current, the reactor atmosphere and the pressures of the used gases greatly affect the size and quality of the graphene. The arc current is varied between 100 and 150 A. The purity and the number of layers of graphene are determined via TG/DTA and the Raman spectroscopy. The optimum synthesis conditions are determined at the electrode diameter of 12 mm and the arc current of 150 A in a He and N_2 atmosphere. Raman spectra and TG/DTA of the synthesized graphene using 12 mm electrode in He and N_2 atmosphere are depicted in Fig. 1.

L_D/L_G ratio which provides the information about graphene purity is obtained as 0.66. It should be between 0 and 1 [19], and L_G/L_{2D} ratio is related to the number of graphene layers and it is calculated as 1.33 which means a few layers (4–5 layers). Fig. 1b shows the TG/DTA graph

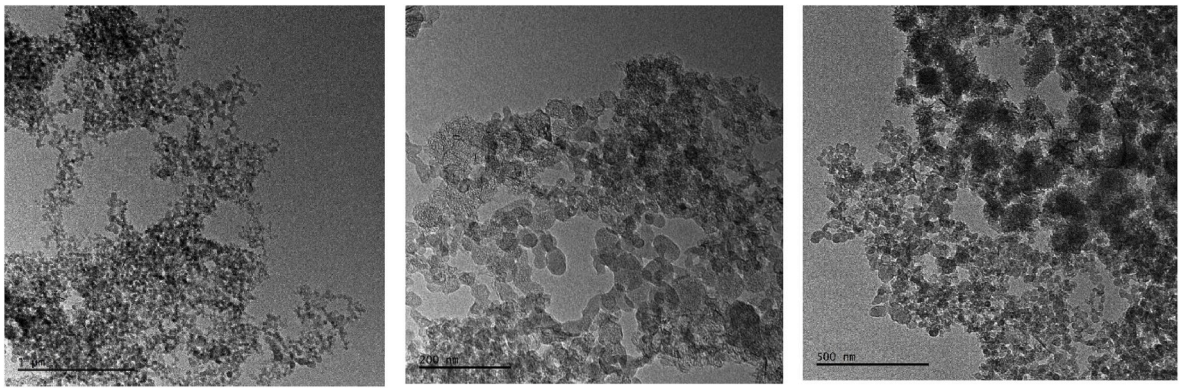

Fig. 2. Bright Field-BF, TEM images at different magnifications of GNF obtained from the 12 mm electrode He and N_2 process gases.

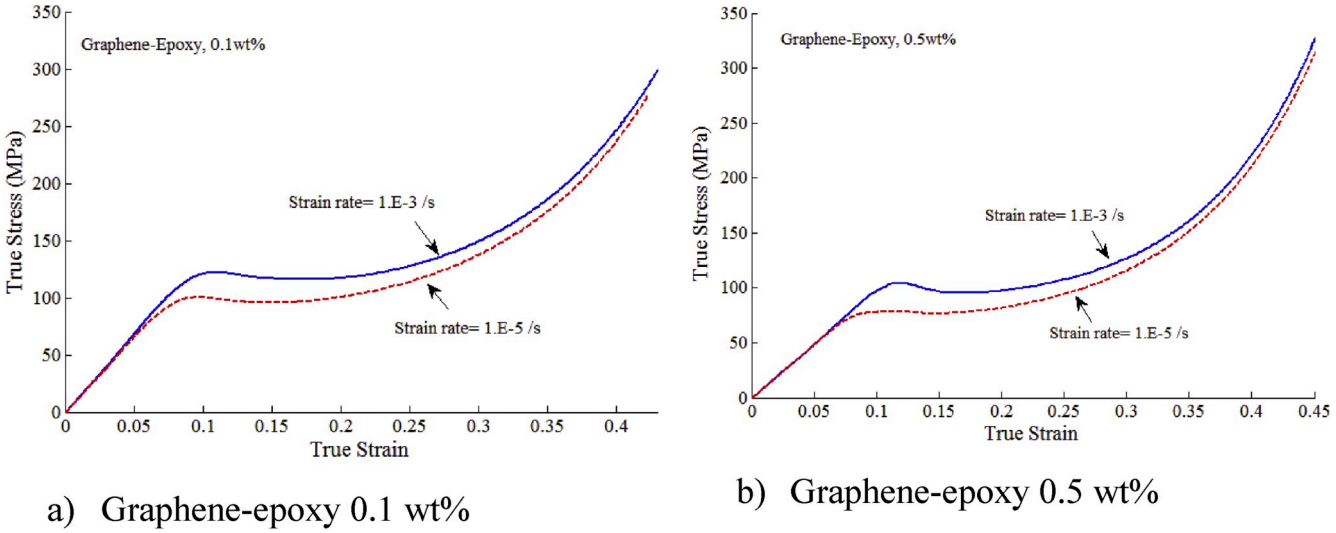

Fig. 3. True stress-strain behaviors of graphene-epoxy with GNF content of 0.1 and 0.5 wt % under quasi static compression tests. Strain rates are 1.E−3 and 1. E−5/s.

of graphene synthesized at 150 A in He and N2 medium using a 12 mm electrode. According to the graph, mass reduction in one step was observed. This result indicates that the graphene produced is of high purity and high crystallinity, [17].

The detailed structural examination of the graphene structure obtained by the electric arc discharge method is carried out in the JEOL JEM 2100 high-resolution HRTEM device in bright field mode. 1 μm, 200 nm and 500 nm images are taken from the sample. TEM images are depicted in Fig. 2.

Fig. 2 shows typical of graphene sheets synthesized by arc discharge technique at 150 A in He and N_2 medium. Neither amorphous carbon nor other carbon structures are observed. TEM images of the synthesized graphene sheets also indicates numerous wrinkles on the surfaces which gives them different levels of transparency.

The specific surface area of Brunauer-Emmet-Teller (BET) is determined by nitrogen adsorption using a Micromeritics TriStar II device at a liquid nitrogen temperature. The BET specific surface area of the graphene produced at a value of 150 A in the He and N_2 atmosphere using the 12 mm electrode is measured as 143.2067 m^2/g. This result shows that BET specific surface area is quite wide compared to graphite (1–20 m^2/g), [17]. The broad BET specific surface area indicates that the graphene which is synthesized has several layers.

3. Fabrication of graphene-epoxy nanocomposite

Due to weak intermolecular van der Waals forces, graphene tends to agglomerate. Therefore, dispersing the graphene into epoxy matrix is always a challenge. Sonication is the main dispersion methods in the manufacturing of nanocomposites. An additional processes such as mechanical stirring and magnetic stirring improve the dispersion process, [20]. In this work, the solution mixing method is used for the preparation of epoxy nanocomposites. Graphene content is not the only factor which influence the properties of graphene-epoxy nanocomposite. The other influential factors are the dispersion method, the usage of solvent, the modification of graphene-surface etc. In this work, acetone is used as solvent. GNF is dispersed in acetone (1 mg/ml) by using sonicator (200 W, 20 KHz, Bandelin Sonopuls HD 3200) for 90 min. The epoxy resin (Fibre Glast 2000, Fibregrast Inc.) is then added and sonicated for another 90 min. Following the sonication, acetone needs to be removed. Therefore, the mixture is heated in a vacuum oven at 70 °C overnight to remove the acetone. Then, epoxy resin curing agent (Fibre Glast 2120, Fibregrast Inc.) is added. The mixing ratio of the epoxy and curing agent is 3:1 as recommended by the manufacturer. The mixture is degassed by stirring under vacuum at room temperature for 60 min. This mixture is poured into a silicon mold and cured in an oven at 60 °C for 24 h, followed by 4 h post-cure at 90 °C, [11]. The graphene-epoxy nanocomposites are prepared for various graphene contents (0.1 and 0.5 wt %). In this work, the functionalization of

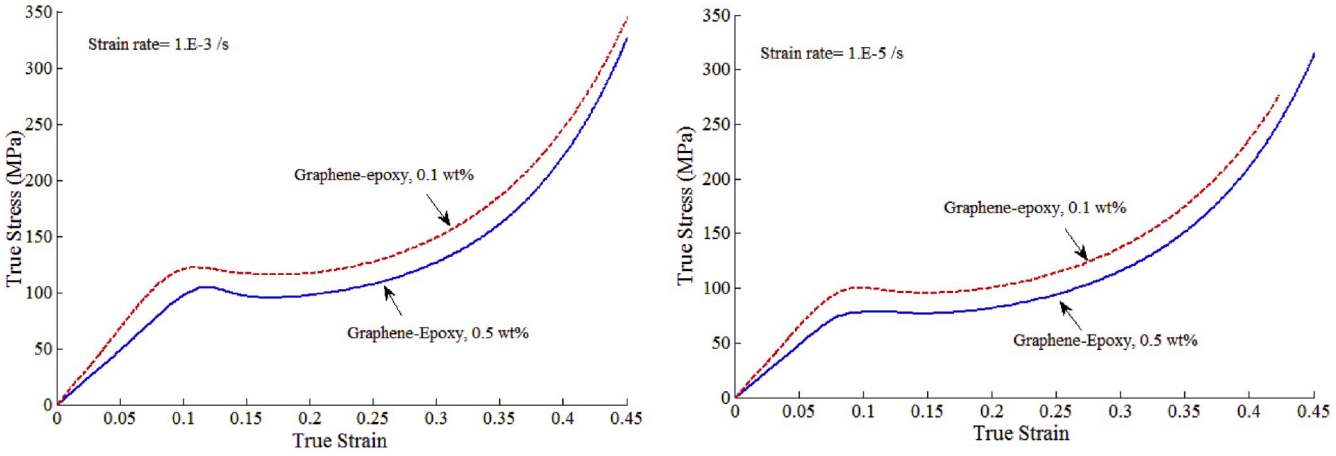

Fig. 4. Comparison of true stress-strain behaviors of graphene-epoxy nanocomposites with GNF content of 0.1 and 0.5 wt% under quasi static compression tests.

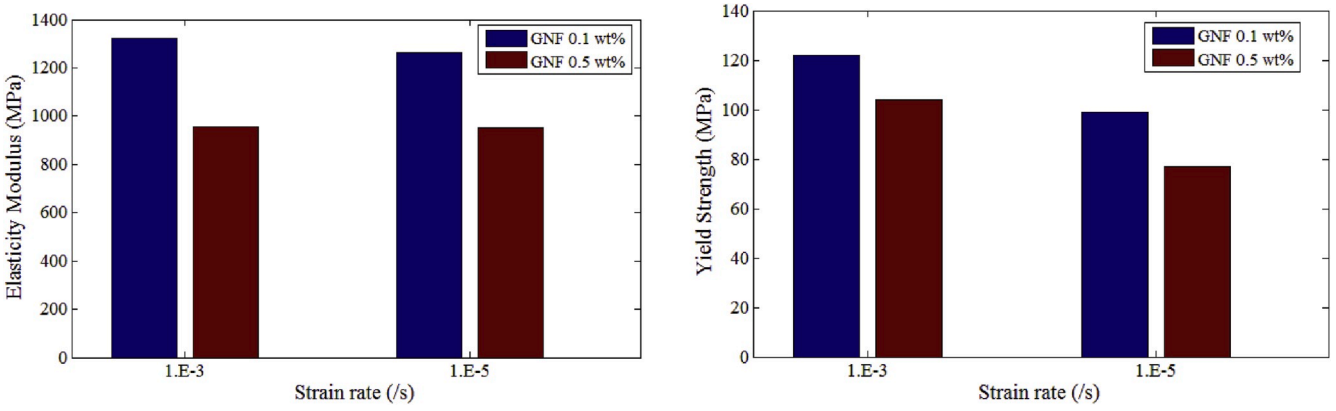

Fig. 5. The mechanical properties (elasticity modulus and yield strength) of graphene-epoxy nanocomposite with GNF content of 0.1 and 0.5 wt under quasi static compression test.

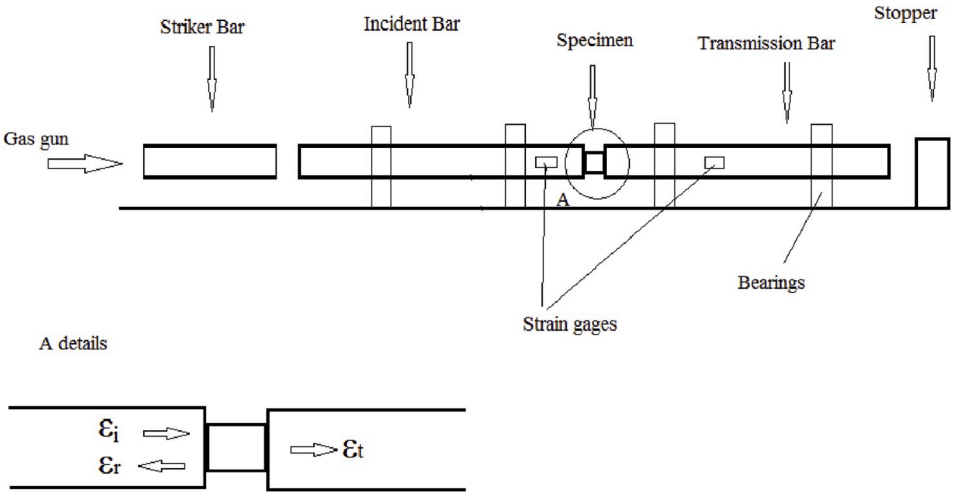

Fig. 6. Schematic of SHPB.

graphene surface is not done. It will be considered in future works in addition to using three roll milling method as an effective way of dispersing the reinforcement into epoxy matrix, [20].

4. Mechanical characterization

4.1. Quasi static compression tests

Uniaxial quasi static compression tests were conducted using an INSTRON 5969 universal testing machine. The tests were carried out at

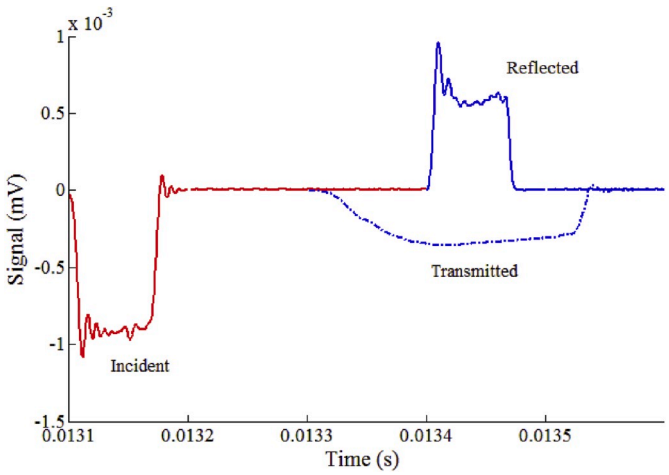

Fig. 7. Incident, reflected and transmitted waves during SHPB test.

the strain rates of 1.E−3 and 1.E−5/s at room temperature. Using the load–displacement data of the testing device, the stress–strain behaviors of graphene-epoxy nanocomposite with two graphene contents (0.1 and 0.5 wt %) were determined. For each loading conditions, at least four samples were tested. No barreling effect is observed due to the low thickness/diameter ratio. True stress-strain behavior of graphene-epoxy with graphene content of 0.1 and 0.5 wt% at two strain rates are depicted in Fig. 3.

In elastic region, a small rate dependency is observed. The elasticity modulus is calculated from the initial slope of the true stress–strain curves. Following the elastic behavior, rate dependent yielding is observed. After yielding, a stress drop at 1. E−3/s strain rate with plastic straining is seen due to the decrease of the internal stress which may result in a rearrangement of molecular defects until a more stable configuration is reached, [21]. When the strain rate is decreased (in the case of 1.E−5/s), softening after yielding almost disappeared. With plastic straining, hardening occurs due the entanglement of the polymer chains. The rate dependency is much more prominent at yielding and viscoplastic region.

For comparison of the influences of GNF contents, the true stress-

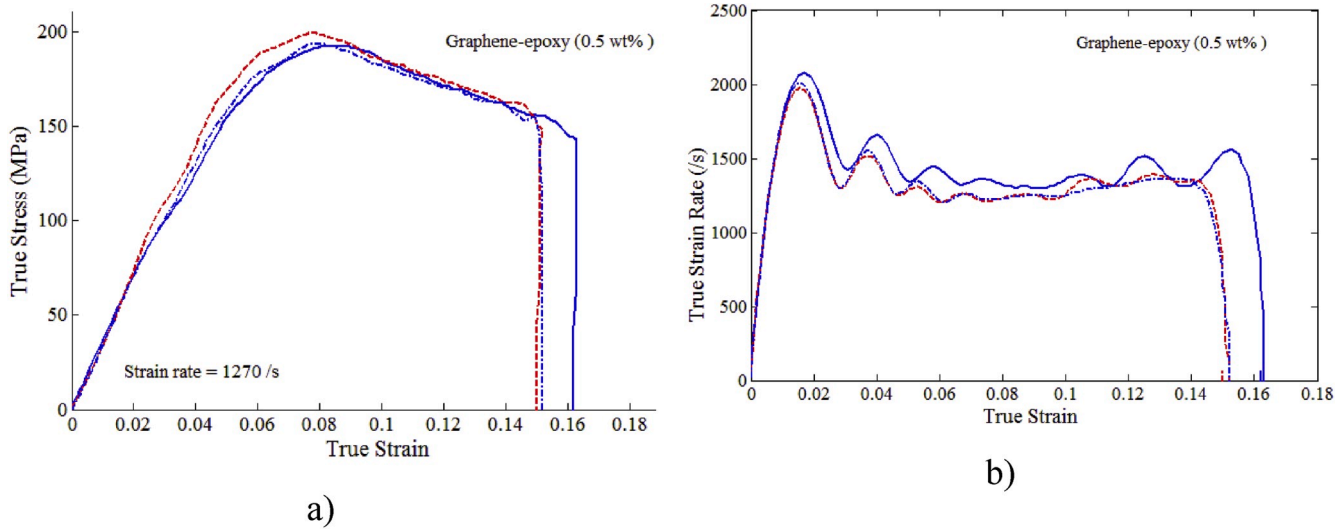

Fig. 8. a. True stress-strain behaviors of repeated experiments on graphene-epoxy (GNF: 0.5 wt%) nanocomposite during SHPB tests, b. Strain rate changes of repeated experiments during the SHPB tests.

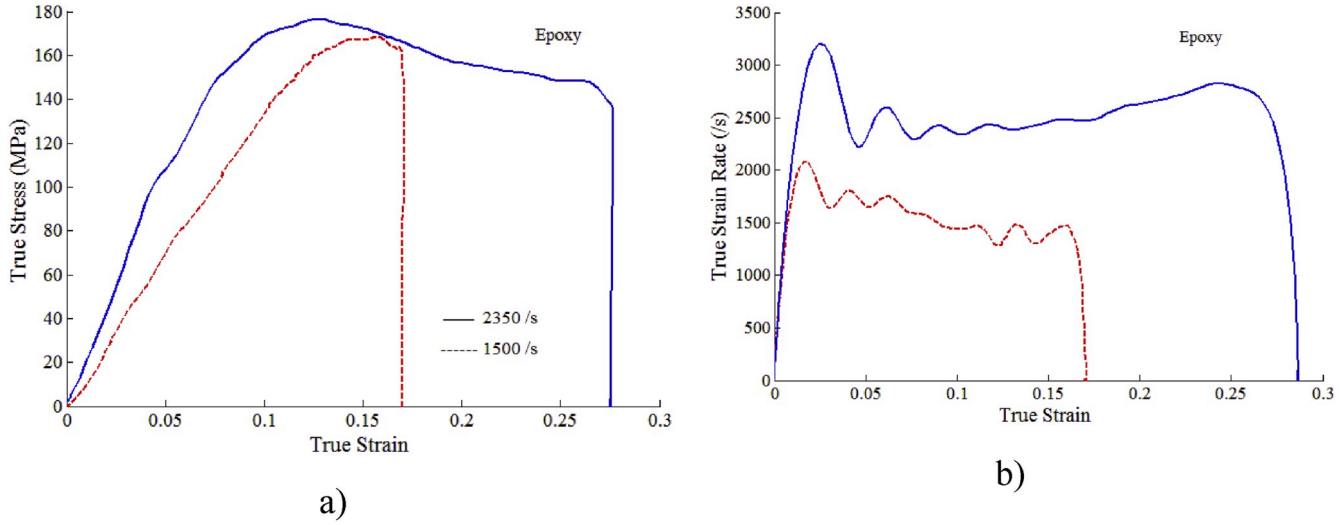

Fig. 9. a. True stress-strain behavior of epoxy at high strain rates of ~1500 and 2350/s during SHPB tests, b. True strain rate versus true strain curves during SHPB tests.

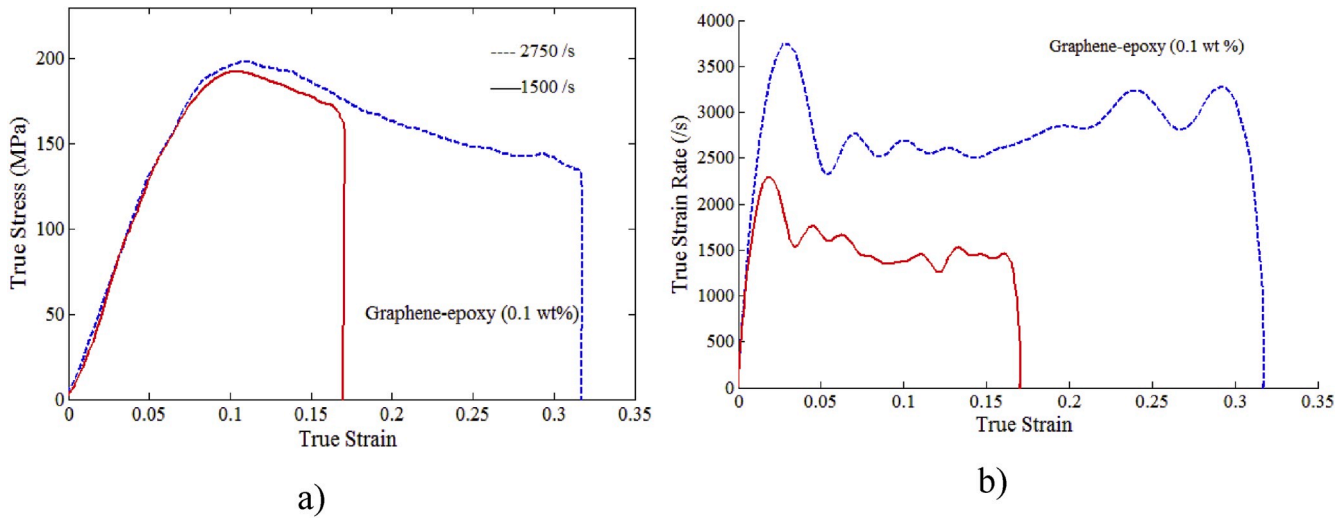

Fig. 10. a. True stress-strain behavior of graphene-epoxy nanocomposite (GNF: 0.1 wt %) at high strain rates of ~1500 and 2750/s. b. Strain rate changes of graphene-epoxy nanocomposite (GNF: 0.1 wt %) during SHPB tests.

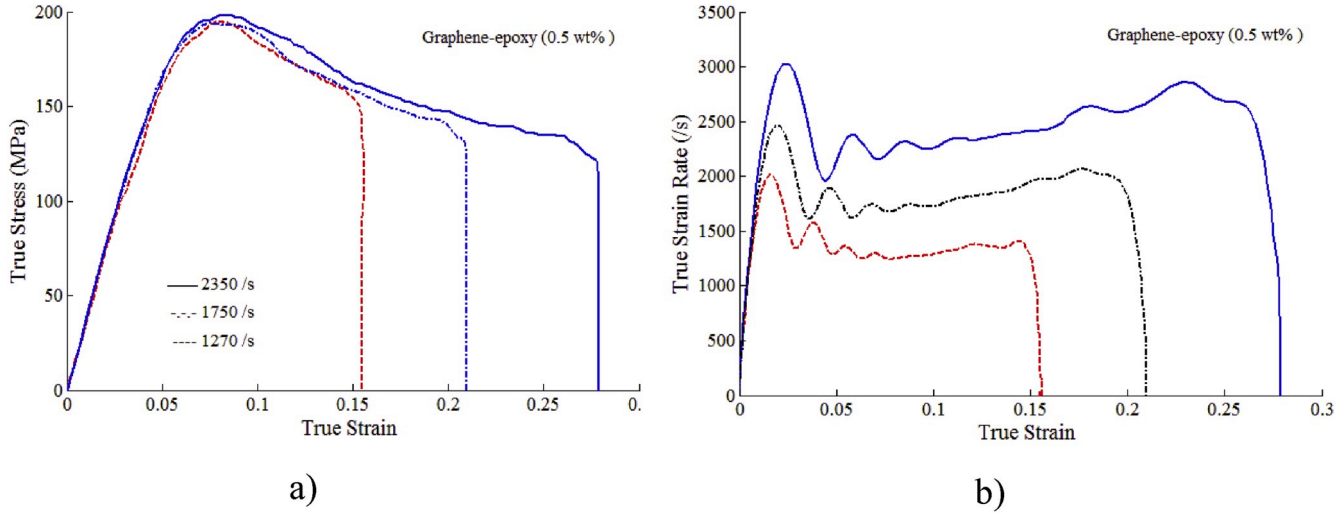

Fig. 11. a. True stress-strain behavior of graphene-epoxy (GNF: 0.5 wt %) at high strain rates of approximately ~1270, 1750 and 2350/s. (SHPB tests) b. Strain rate changes during SHPB tests.

strain curves are plotted for 0.1 and 0.5 wt% graphene content and the results are depicted in Fig. 4.

Increasing the GNF contents leads to a decrease in the mechanical properties due to probably agglomeration of the graphene in the structure. The mechanical properties of graphene-epoxy nanocomposite under quasi static compression are depicted in Fig. 5.

4.2. Dynamic uniaxial compression tests

Since, the conventional servo-hydraulic machine is limited to lower strain rates (<10/s), for high strain rate testing, the Split-Hopkinson Pressure Bar (SHPB) is used commonly. The strain rates as high as 1. E2 to 1.E4/s can be obtained in SHPB. The working principle of SHPB is based on one dimensional wave propagation. It consists of a gas gun, a striker bar, an incident bar and a transmission bar, (Fig. 6). The sample tested is sandwiched between the incident and transmission bar. All bars are made of the same material with the same cross section area. During the test, at all times, the striker, incident and transmission bar should remain elastic.

When the striker bar is propelled by gas pressure, compressive stress wave is generated and propagated toward the incident bar. When the wave arrives at the interface between the incident bar and the specimen, the part of the wave is reflected back into the incident bar and the rest transmits through the specimen into the transmission bar. By varying the impact velocity and specimen size, different strain rates can be achieved.

Strain gauges mounted on each bar in the form of half Wheatstone bridge measure only the axial strain and remove the effect of any bending. The elastic strain generated in incident and transmission bar are used to calculate the stress-strain in the sample. The nominal strain rate in sample is proportional to the reflected strain and inversely proportional to the length of specimen and is calculated as

$$\dot{\varepsilon}(t) = -\frac{2C_o}{L}\varepsilon_r(t) \quad (1)$$

where C_o is the wave velocity of the bar material, L is the initial length of the specimen, $\varepsilon_r(t)$ is the time-resolved strain associated with the reflected pulse in the incident bar. Considering the elasticity modulus (E) and density (ρ) of the bars, the wave velocity of the bar is $C_o = \sqrt{E/\rho}$. The nominal stress is calculated according to 3 wave analysis as,

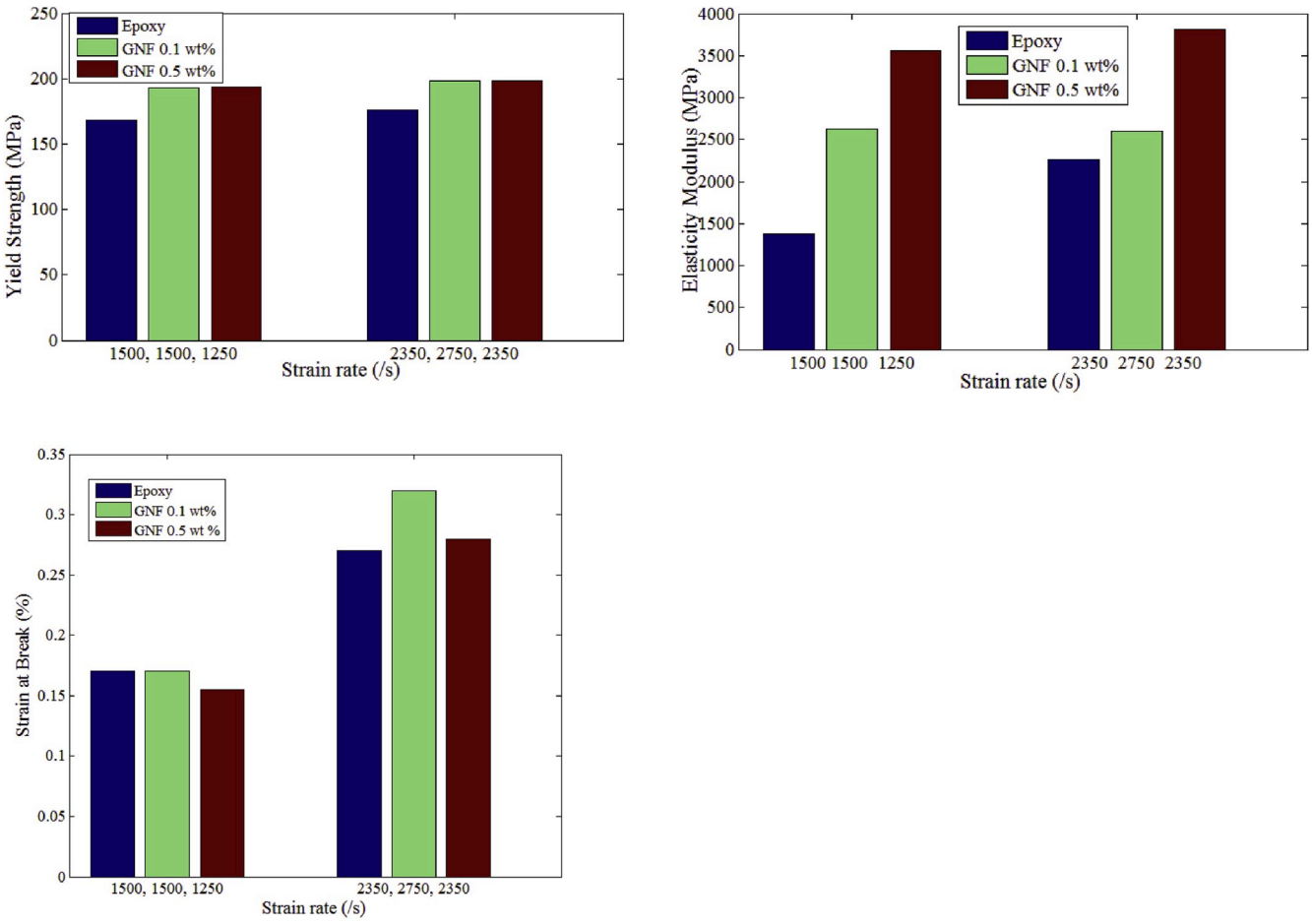

Fig. 12. The mechanical properties of epoxy and graphene-epoxy under dynamic loading (SHPB tests).

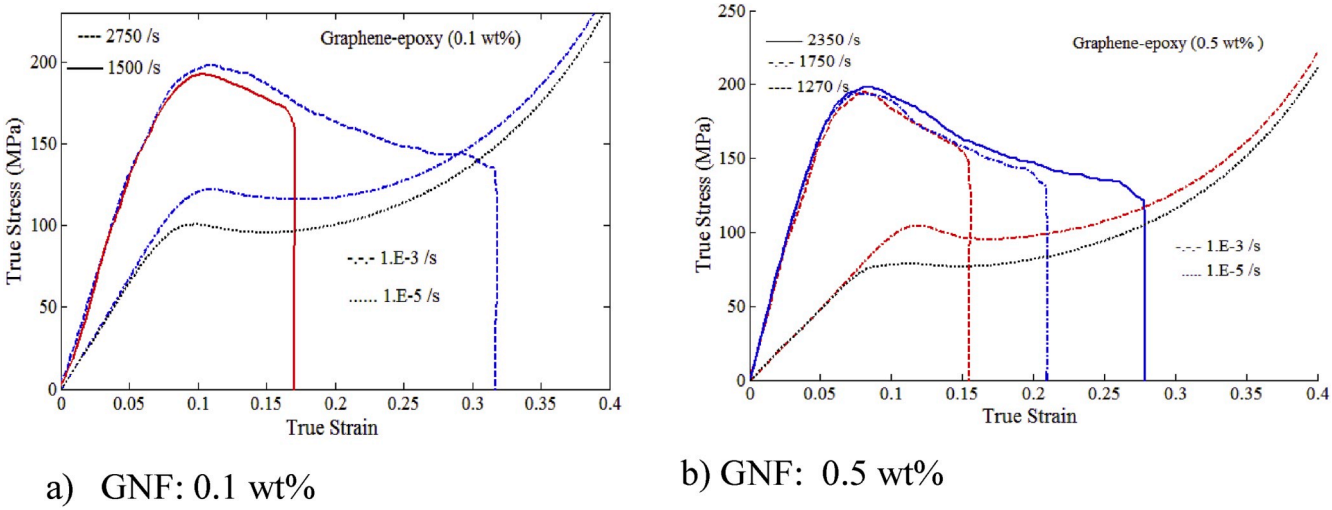

a) GNF: 0.1 wt%

b) GNF: 0.5 wt%

Fig. 13. True stress–true strain curves of graphene-epoxy nanocomposite under uniaxial quasi-static compression loading and dynamic compressive loadings (SHPB) at room temperature.

$$\sigma(t) = \frac{A_t}{2A_s} E[\varepsilon_i(t) + \varepsilon_r(t) + \varepsilon_t(t)] \tag{2}$$

where A_s and A_t are the cross-section areas of the specimen and transmission bar respectively, $\varepsilon_i(t)$ is the time-resolved strain associated with the incident pulse in the incident bar, $\varepsilon_t(t)$ is the time-resolved axial strain in the transmission bar and E is Young's modulus of the bar. True strain and stress are identified from nominal measurements as

$$\varepsilon_t(t) = -\ln(1 + \varepsilon_n(t)) \tag{3}$$

$$\sigma_t(t) = \sigma_n(t)[1 - 2\nu\varepsilon_n(t)]$$

A typical pulse signal recorded using strain gauges on incident and transmission bars are given in Fig. 7.

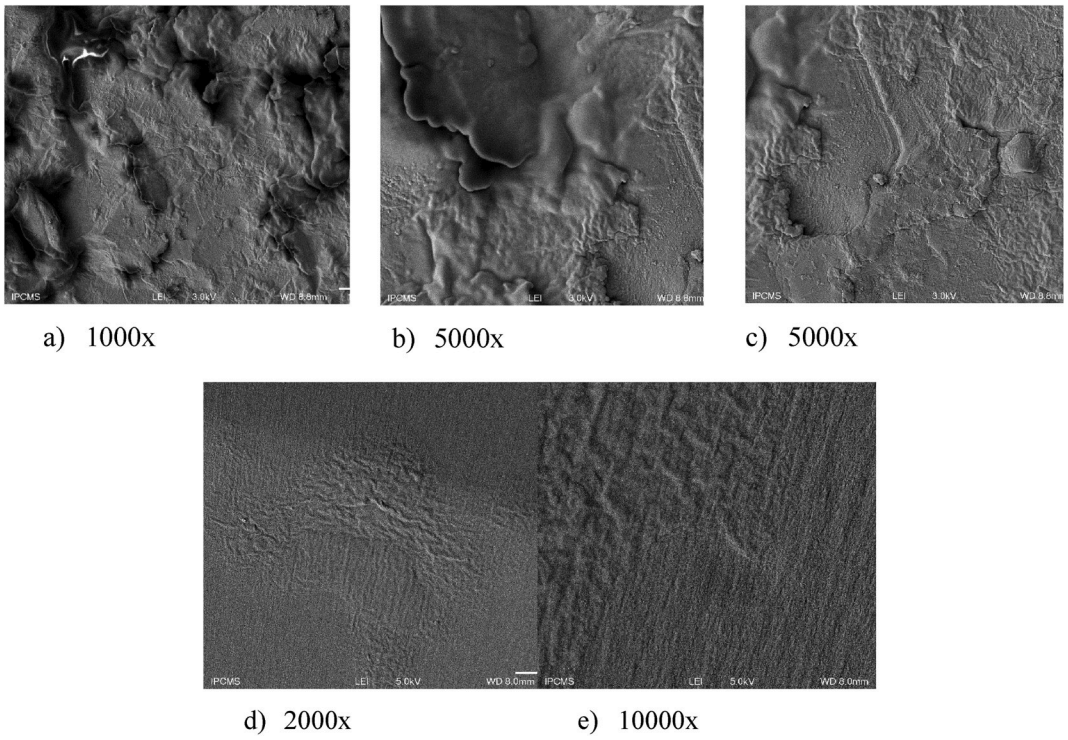

Fig. 14. SEM micrographs of fractured surfaces of neat epoxy under SHPB test.

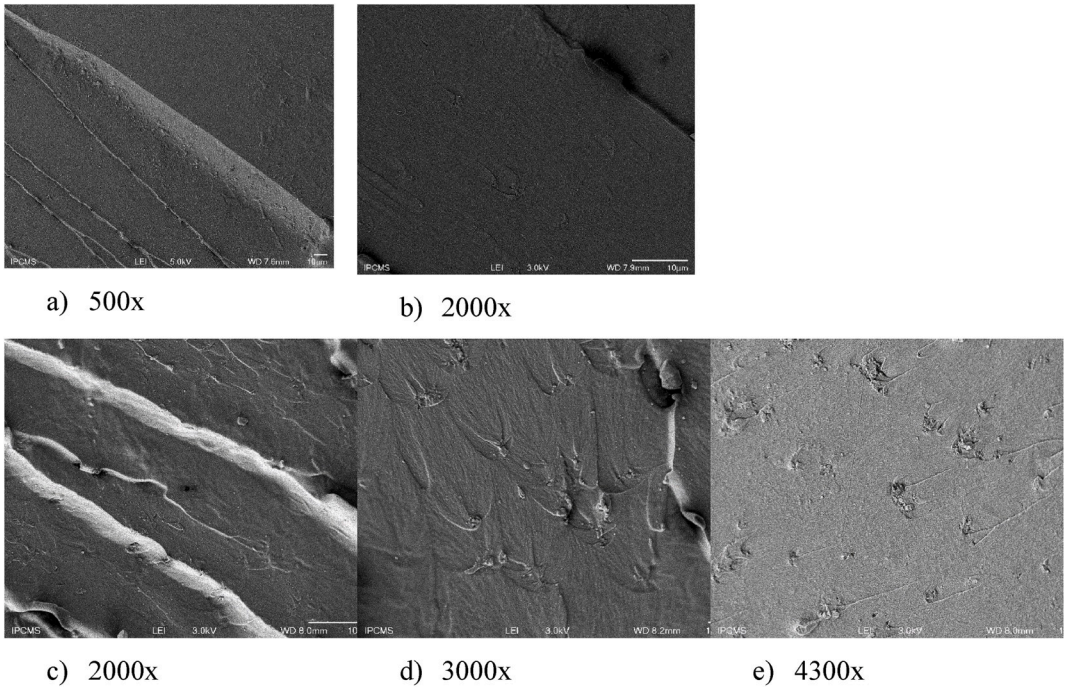

Fig. 15. SEM micrographs of fractured surfaces of graphene-epoxy nanocomposites (GNF: 0.1 wt %) (a–b) and (GNF: 0.5 wt %) (c–e) under SHPB test.

The experiments are repeated at least three times for each loading conditions for epoxy and graphene-epoxy nanocomposites. True stress-strain behaviors of graphene-epoxy (0.5 wt%) for three repeated tests and strain rate changes during these tests are depicted in Fig. 8. Coincided curves indicate their repeatability and consistency. Strain softening after peak stress is observed as seen in Fig. 8.

The true stress strain curves of epoxy for ~1500 and 2350/s strain rates are shown in Fig. 9. Visco-elastic behavior is observed. Following the yield, strain softening behavior is observed at 2350/s strain rate.

True stress-strain behaviors of graphene-epoxy with 0.1 and 0.5 wt% GNF at various high strain rates are depicted in Figs. 10 and 11. Elastic behavior is almost linear. Following the yielding, strain softening is observed for all cases. Yield behavior and subsequent behaviors are rate dependent. Increasing the strain rate yields an increase in the yield stress and the strain at break.

The mechanical properties upon the addition of GNF are seen in

Fig. 12. The strain rate dependent mechanical behavior is observed as expected. The yield strength is increasing with an increase in GNF content and as well as with an increase in strain rate as seen in Fig. 12. Similarly, the elasticity modulus has the same trend. However, compared to the yield strength, the enhancement in the elasticity modulus with the addition of GNF is much more prominent.

The strain rates were observed over a range of 1500–2750/s during the impact testing of nanocomposites. At the strain rate of 2350/s, the maximum strength was achieved by the GNF-epoxy with 0.5 wt% is about 200 MPa which correspond to a 12.5% increase compared to the neat epoxy. Various factors such as the interfacial adhesion, the strength of the matrix material and the dispersion of particles in the matrix influence the strength of the nanocomposites. The dispersion of the GNP in the polymer matrix is one of the most crucial factors to be considered. Agglomeration of nanoparticles in polymers induce the local stress concentration, and reduce the particle matrix adhesion, and thus weaken the load transfer efficiency at the interface. The preparation of nanocomposites without agglomeration by the commonly-used solution mechanical mixing techniques is difficult. Therefore, the increase in the strength of nanocomposite compared to neat epoxy is not very high.

GNF-epoxy with 0.5 wt % shows that the highest elasticity modulus. It is achieved by a 68.2% increase compared to the neat epoxy which was 2266 MPa at 2350/s strain rate. The maximum stress is increased from 176 MPa to 198 MPa with a reinforcement of 0.5 wt% of GNF filler. At high strain rates, the strain at break does not decrease with the introduction of GNF, even though aggregated reinforcements are known to act as failure points during the elongation of a composite material [17]. To observe the prominent effect of strain rate, the comparison of quasi static and high strain rate experimental results are done in Fig. 13.

As seen in Fig. 13, the yield strength of the nanocomposite is almost doubled at high strain rates compared to the quasi static loading. The elasticity modulus is around 2600 and 3800 MPa for graphene-epoxy with 0.1 and 0.5 wt% GNF respectively at high strain rate tests, while it is around 1390 and 950 MPa at quasi static loadings. The strain rate effect can be associated with the molecular motion of the polymer chains. At high strain rates, the molecular motion of the chains are restricted. There is no time for rearrangement of polymer chains on the time scale of the high strain rate tests. Since the fundamental process of yielding of amorphous polymers consists of the jump of macromolecule segments from one equilibrium position to another [22], at a higher strain rate, there is a higher molecular resistance to jumps and, hence, a higher yield stress is observed.

4.3. Scanning electron microscopy (SEM) fractography

To obtain much more information about the interfacial adhesion between GNP fillers and epoxy matrix, the fracture surfaces of composites are investigated by SEM and depicted in Figs. 14 and 15. The cleavages are observed on the fracture surfaces of epoxy and nanocomposites. As seen in Fig. 14, deep cleavages are observed in neat epoxy specimens, whereas shallow cleavages are observed in nanocomposites (Fig. 15-d).

The SEM micrograph (Fig. 14 (d, e)) shows smooth and featureless fracture surface for the neat epoxy specimen tested at SHPB. This type of morphology indicates a typical brittle fracture behavior of epoxy resin [12,23].

After addition of nanoparticles, the fracture surfaces show rough fractographic features, river like markings, and graphene agglomerates. When the GNF content is increased (Fig. 15(d–f)), the fracture surfaces show more and deeper river markings around the agglomerates. The stress concentrations are developed around the agglomerated particles and the failure is initiated at these localized domains [12,24]. Micro-voids are observed in GNF-epoxy nanocomposites containing higher graphene content (Fig. 15(d–f)). Compared to epoxy, the failure mode is significantly changed in GNF-nanocomposite as shown in Figs. 14 and 15.

5. Results and discussions

The aim of this work is to synthesis of GNF, manufacturing of nanocomposite and characterization of GNF-epoxy nanocomposite at quasi static and high strain rates which are observed in a variety of applications such as crash of vehicles, bullet proof armors and impact of the structures. High purity GNF are synthesized by using the electric arc discharge technique. Synthesized GNF are characterized by TG/DTA, Raman spectroscopy, BET and TEM techniques. Raman spectra of synthesized GNF reveal multiple of layers and high purity as well as BET. According to TG/DTA, mass reduction in one step is observed. This result indicates that the graphene produced is of high purity and high crystallinity.

The solution mixing manufacturing process is used to fabricate GNF-epoxy nanocomposites. Apart from many works in the literature, the high strain rate behavior of graphene-epoxy nanocomposite is investigated in addition to quasi static behavior. High strain rate behaviors of graphene-epoxy nanocomposites with 0.1 and 0.5 wt% GNF content were investigated using SHPB at the strain rates up to 2750/s. Graphene-epoxy with 0.5 wt % GNF shows that the highest elasticity modulus. 68.2% increase in the elasticity modulus is observed at 2350/s strain rate. 12.5% increase in the strength under impact loading of the graphene-epoxy nanocomposite using 0.5 wt% GNF is obtained as compared to the neat epoxy at the strain rate of 2350/s.

Quasi static compression tests are performed at 1.E−3 and 1.E−5/s strain rates for GNF-epoxy with 0.1 and 0.5 wt%. As expected increasing strain rate leads to an increase in the elasticity modulus and the yield strength. Comparing the experimental results at high and quasi static loading conditions reveals that the yield strength of the material is doubled under dynamic loading conditions. Both the pure epoxy and graphene-epoxy nanocomposites exhibit strain rate dependent behavior in the tested strain rates of 1.E−3/s to 2750/s. Rate dependent elasticity modulus, yield strength and post yield behavior is associated with the changes in the molecular mobility of the polymer chains with strain rate.

The achievement of maximum improvement in the mechanical properties of graphene-epoxy nanocomposites, depends on the dispersion method, the usage of solvent, surface modification of GNF etc. As mentioned previously, graphene tends to agglomerate due to the weak van der Waals interactions. In future works, to handle the limited dispersibility and interfacial bonding of graphene, the surface modifications will be carried out. Also, it is planned to use three roll milling process for dispersing GNF into epoxy matrix since it involves high shear stresses, [20].

Declaration of competing interest

There is no conflict of interest to declare about the manuscript titled ‘High strain rate behavior of graphene-epoxy nanocomposites’ by Özgen U. Colak, Nadia Bahlolui, Deniz Uzunsoy and Charles Francart.

Acknowledgement

We thank to CNRS, IPCMS for SEM images and Cantekin Kaykılarlı from Bursa Technical University for the preparation of nanocomposite specimens.

References

[1] C.R. Siviour, J.L. Jordan, High strain rate mechanics of polymers: a review, J. Dyn. Behav. Mater. 2 (2016) 15–32.
[2] E.M. Arruda, M.C. Boyce, R. Jayachandran, Effects of strain rate, temperature and thermomechanical coupling on the finite strain deformation of glassy polymers, Mech. Mater. 19 (2) (1995) 193–212.
[3] K.S. Novoselov, Nobel lecture: graphene: materials in the flatland, Rev. Mod. Phys. 83 (3) (2011) 37–49.
[4] G. Wang, B. Wang, L. Park, Y. Wang, B. Sun, J. Yao, Highly efficient and large-scale synthesis of graphene by electrolytic exfoliation, Carbon 47 (14) (2009) 42–46.

[5] C. Su, A. Lu, Y. Xu, F. Chen, A.N. Khlobystov, L. Li, High-quality thin graphene films from fast electrochemical exfoliation, ACS Nano 5 (3) (2011) 32–39.
[6] R.S. Edwards, K.S. Coleman, Graphene synthesis: relationship to applications, Nanoscale 5 (1) (2013) 38–51.
[7] D.G. Papageorgiou, I.A. Kinloch, R.J. Young, Mechanical properties of graphene and graphene-based nanocomposites, Prog. Mater. Sci. 90 (2017) 75–127.
[8] U. Cotul, E.D.S. Parmak, C. Kaykilarli, O. Saray, O. Colak, D. Uzunsoy, Development of high purity, few-layer graphene synthesis by electric arc discharge technique, Acta Phys. Pol., A 134 (2018) 289–291.
[9] S. Shadlou, B. Ahmadi-Moghadam, F. Taheri, The effect of strain-rate on the tensile and compressive behavior of graphene reinforced epoxy/nanocomposites, Mater. Des. 59 (2014) 439–447.
[10] S. Chhetri, N.C. Adak, P. Samanta, N.C. Murmu, T. Kuila, Functionalized reduced graphene oxide/epoxy composites with enhanced mechanical properties and thermal stability, Polym. Test. 63 (2017) 1–11.
[11] E. Topal, E.D. Sam Parmak, D. Uzunsoy, O. Colak, Investigation of mechanical properties of graphene and reduced graphene oxide reinforced epoxy matrix composites, J. Test. Eval. 45 (2017) 1182–1191.
[12] S. Gurusideswar, R. Velmurugan, N.K. Gupta, High strain rate sensitivity of epoxy/clay nanocomposites using non-contact strain measurement, Polymer 86 (2016) 197–207.
[13] Y. Tian, H. Zhang, J. Zhao, T. Li, B. Bie, S. Luo, Z. Zhang, High strain rate compression of epoxy based nanocomposites, Composites Part A 90 (2016) 62–70.
[14] H. Jung, H.K. Choi, H. Lee, Y. Kim, J. Yu, High strain rate effects on mechanical properties of inductively coupled plasma treated carbon nanotube reinforced epoxy composites, Composites Part B 154 (2018) 209–215.
[15] Y. Miao, H. Liu, T. Suo, Y. Mai, F. Xie, Y. Li, Effects of strain rate on mechanical properties of nanosilica/epoxy, Composites Part B 96 (2016) 119–124.
[16] S.A. Bansal, A.P. Singh, S. Kumar, High strain rate behavior of epoxy graphene oxide nanocomposites, Int. J. Appl. Mech. 10 (2018).
[17] Y. Chen, H. Zhao, L. Sheng, L. Yu, K. An, J. Xu, Y. Ando, X. Zhao, Mass-production of highly-crystalline few-layer graphene sheets by arc discharge in various H2–inert gas mixtures, Chem. Phys. Lett. 538 (2012) 72–76.
[18] N. Li, Z. Wang, K. Zhao, Z. Shi, Z. Gu, S. Xu, Large scale synthesis of N-doped multi-layered graphene sheets by simple arc-discharge method, Carbon 48 (2010) 255–259.
[19] G. Wang, B. Wang, J. Park, Y. Wang, B. Sun, J. Yao, Highly efficient and large-scale synthesis of graphene by electrolytic exfoliation, Carbon 47 (2009) 3242–3246.
[20] R. Atif, I. Shyha, F. Inam, Mechanical, thermal, and electrical properties of graphene-epoxy nanocomposites-a review, Polymers 8 (281) (2016) 1–37.
[21] M. Boyce, D. Parks, A. Argon, Large inelastic deformation of glassy polymers. Part 1: rate dependent constitutive model, Mech. Mater. 7 (1988) 13–33.
[22] H. Eyring, Viscosity, plasticity, and diffusion as examples of absolute reaction rates, J. Chem. Phys. 4 (1936) 283–291.
[23] S. Zainuddin, M.V. Hosur, Y. Zhou, A.T. Narteh, A. Kumar, S. Jeelani, Experimental and numerical investigations on flexural and thermal properties of nano clay epoxy nanocomposites, Mater. Sci. Eng. A 527 (2010) 7920–7926.
[24] S. Chhetri, N.C. Adak, P. Samanta, N.C. Murmu, T. Kuila, Functionalized reduced graphene oxide/epoxy composites with enhanced mechanical properties and thermal stability, Polym. Test. 63 (2017) 1–11.